ELECTRONIC SUPPLEMENTARY INFORMATION

(Photo)electrocatalysis of molecular oxygen reduction by S-doped graphene decorated with a star-shaped oligothiophene

Anastasios Stergiou,* Dimitris K. Perivoliotis and Nikos Tagmatarchis*

Theoretical and Physical Chemistry Institute, National Hellenic Research Foundation, 48 Vassileos Constantinou Avenue, 11635 Athens, Greece. E-mail: astergiou@eie.gr (A. Stergiou); tagmatar@eie.gr (N. Tagmatarchis).

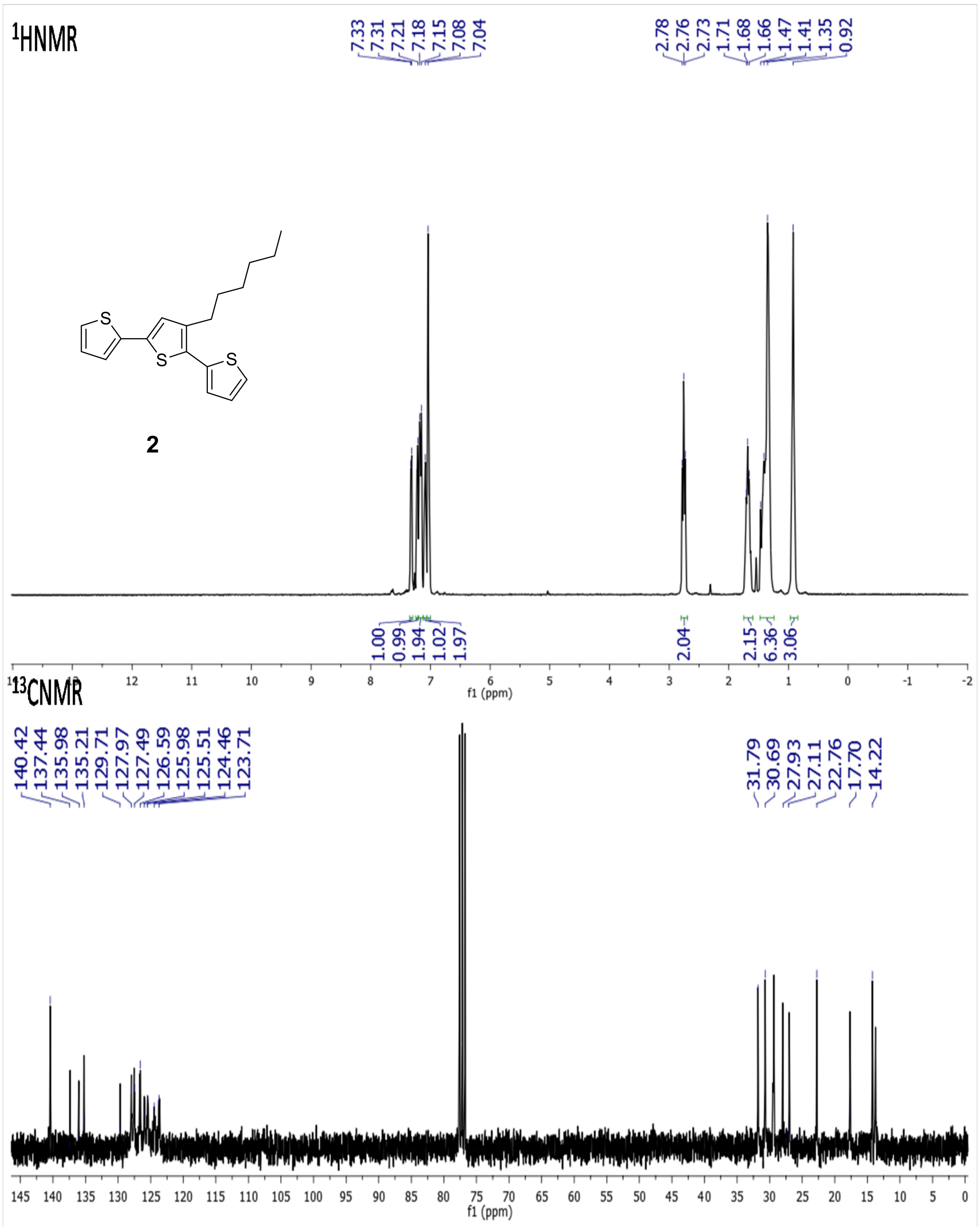

Figure S1. ^{1}H and ^{13}C NMR spectra of compound **2** obtained in $CDCl_3$.

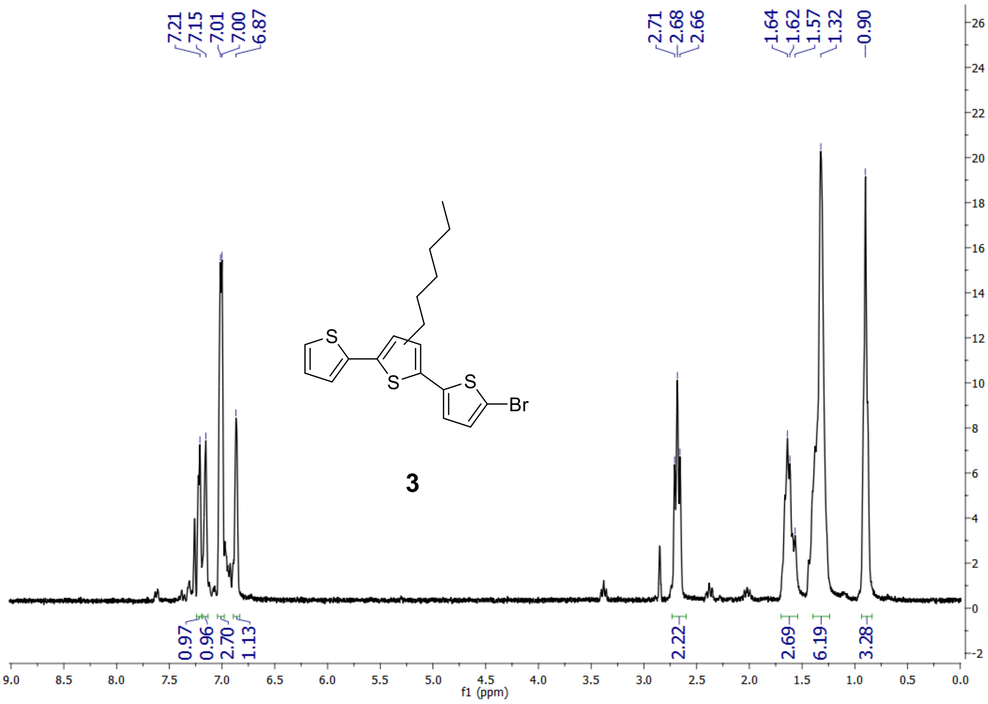

Figure S2. ^{1}H NMR spectrum of compound **3** obtained in $CDCl_3$.

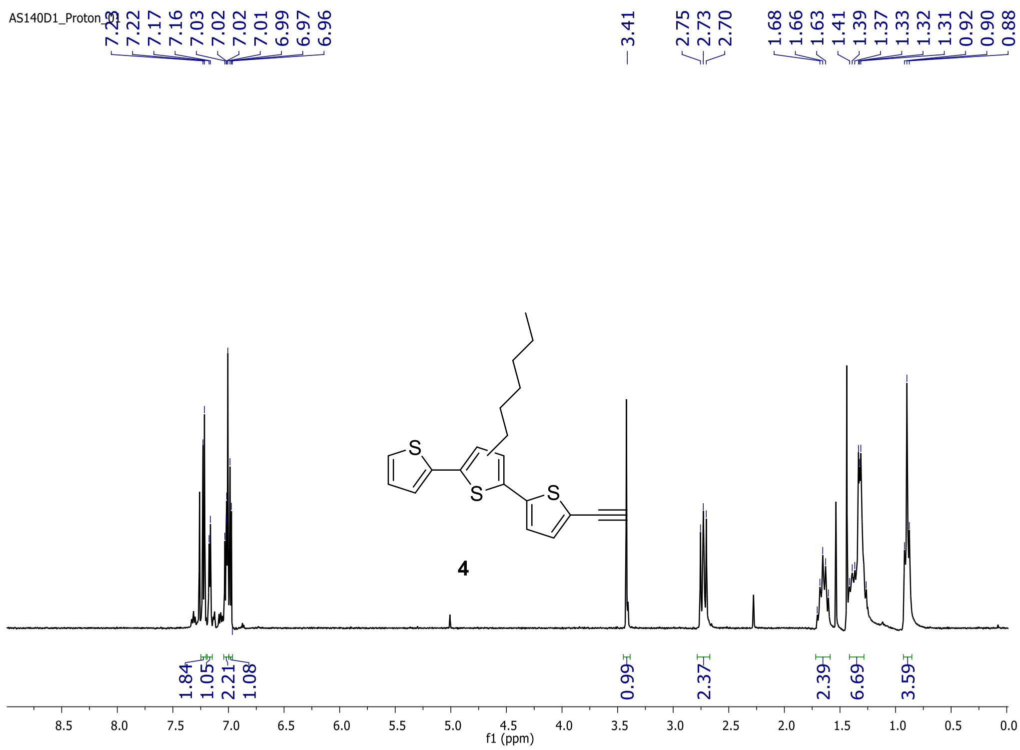

Figure S3. ^{1}H NMR spectrum of compound **4** obtained in $CDCl_3$.

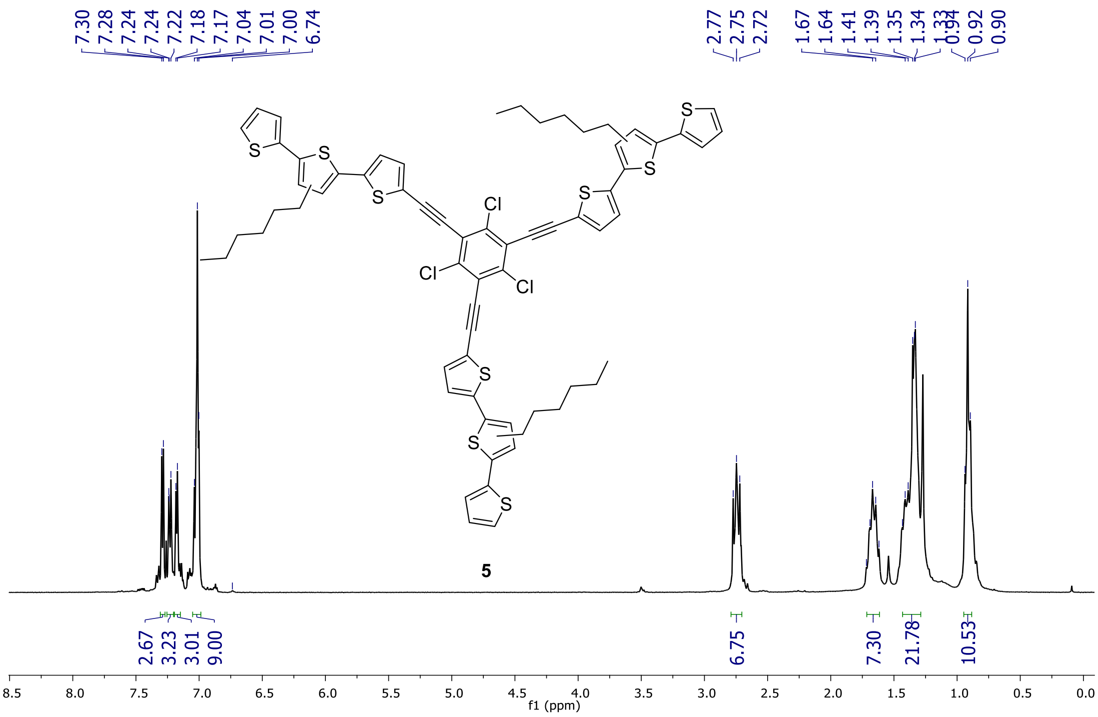

Figure S4. ^{1}H NMR spectrum of star-shaped compound **5** obtained in $CDCl_3$.

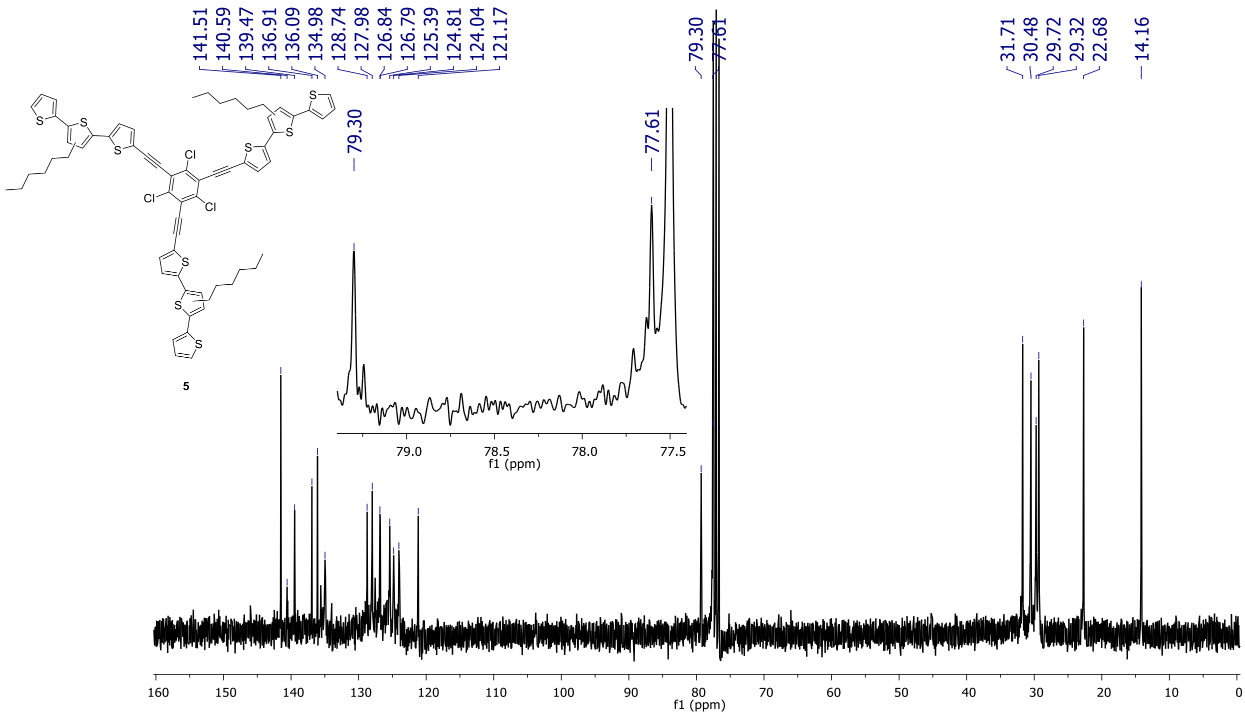

Figure S5. ^{13}C NMR spectrum of compound **5** obtained in $CDCl_3$.

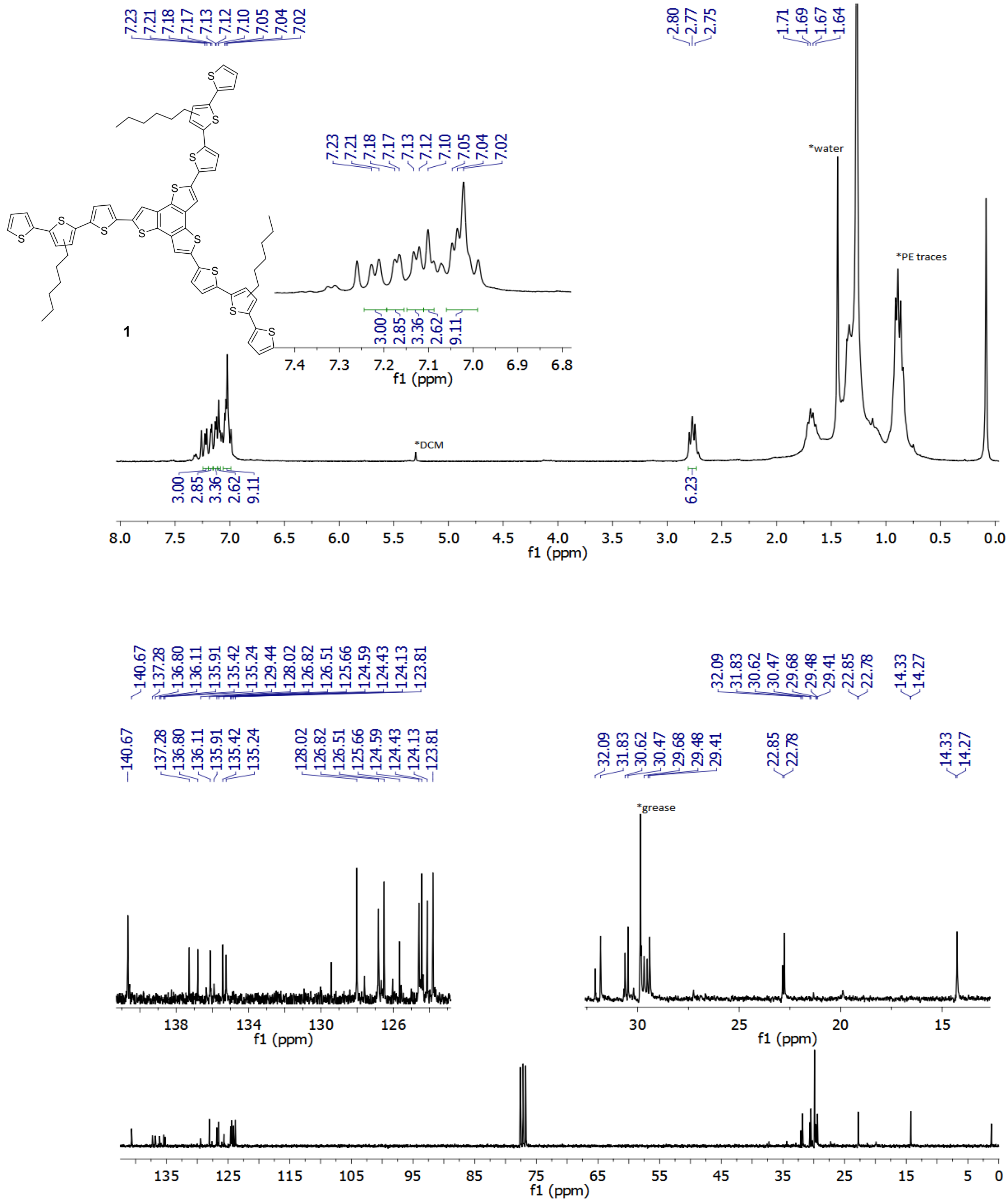

Figure S6. ^{1}H and ^{13}C NMR spectra of star-shaped oligothiophene **1** obtained in $CDCl_3$.

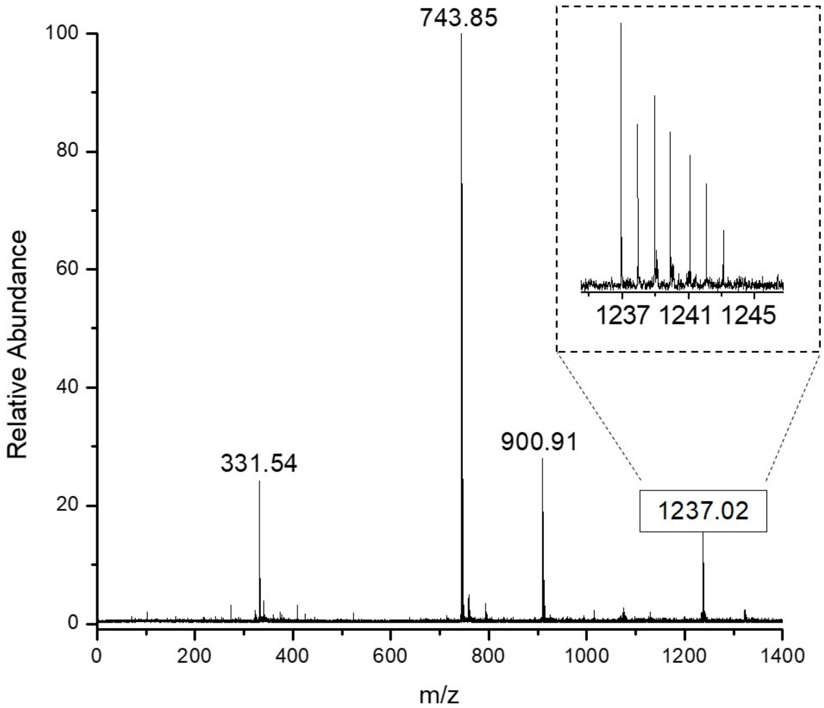

Figure S7. MALDI-TOF mass spectrum of oligothiophene **1**.

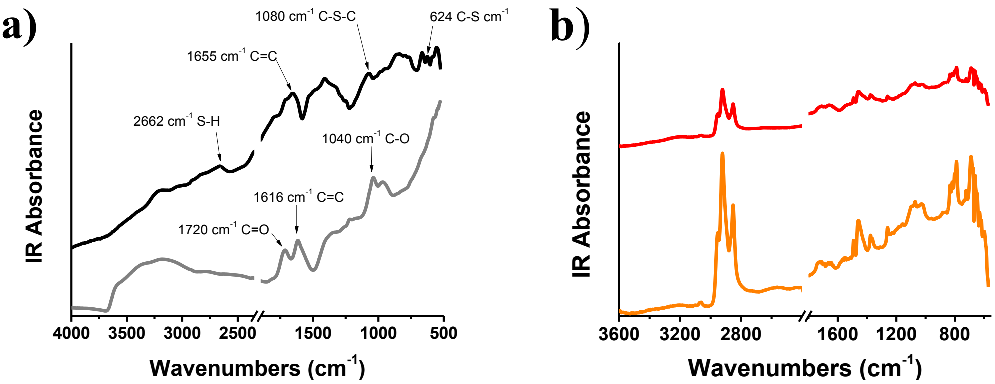

Figure S8. ATR-IR spectra of (a) **GO** (grey) and **SG** (black), and (b) **1** (orange) and **1**/**SG** (red).

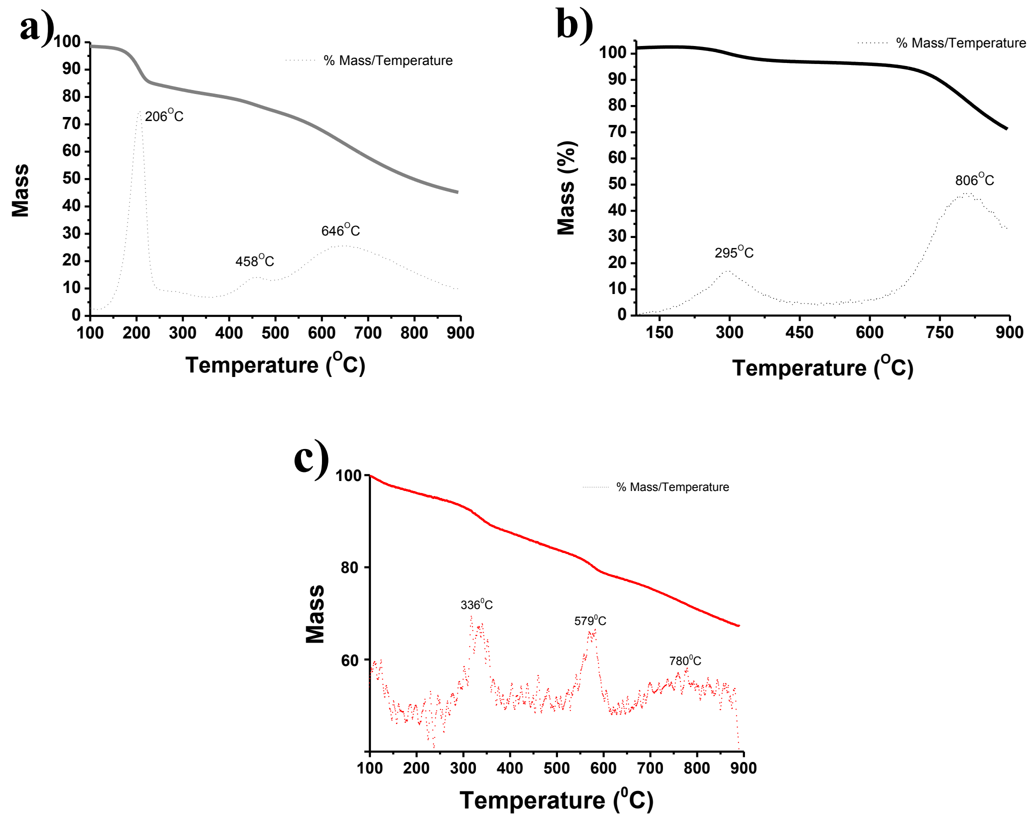

Figure S9. TGA graphs of (a) **GO** (grey), (b) **SG** (black) and (c) **1/SG** (red). Dotted lines represent the first derivative of mass/temperature.

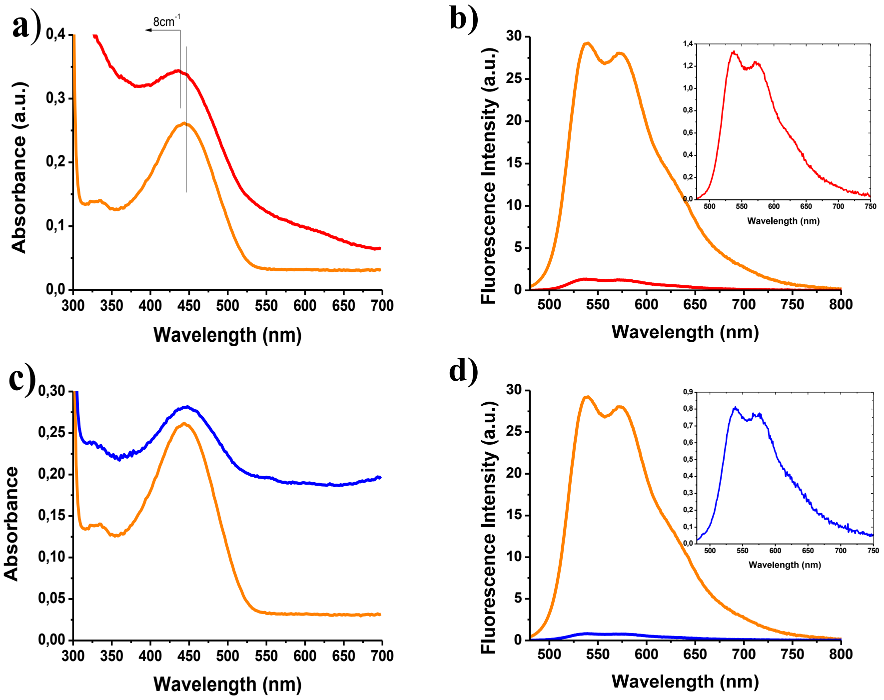

Figure S10. (a) UV-Vis and (b) fluorescence emission (λ_{exc} 441 nm) spectra of **1** (orange) and **1/SG** (red) recorded in benzonitrile. (c, d) UV-Vis and fluorescence emission (λ_{exc} 441 nm) spectra of reference **1/GO** (blue). The insets of (b, d) represent the magnified fluorescence emission intensity of the ensembles.

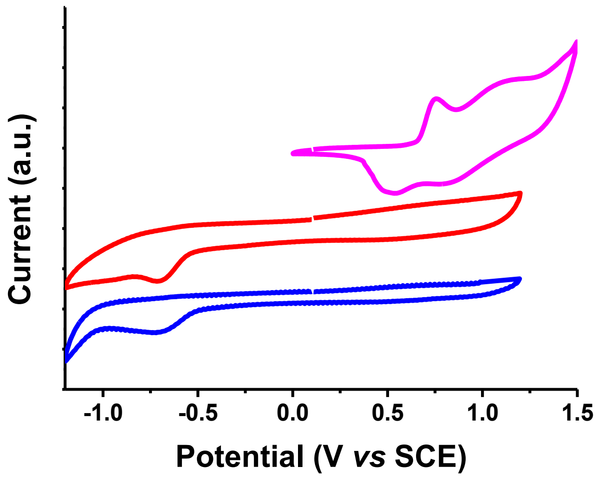

Figure S11. CV of **1** (magenta), **1/SG** (red) and **1/GO** (blue) in N_2-saturated 0.1 M $TBAPF_6$ in benzonitrile.

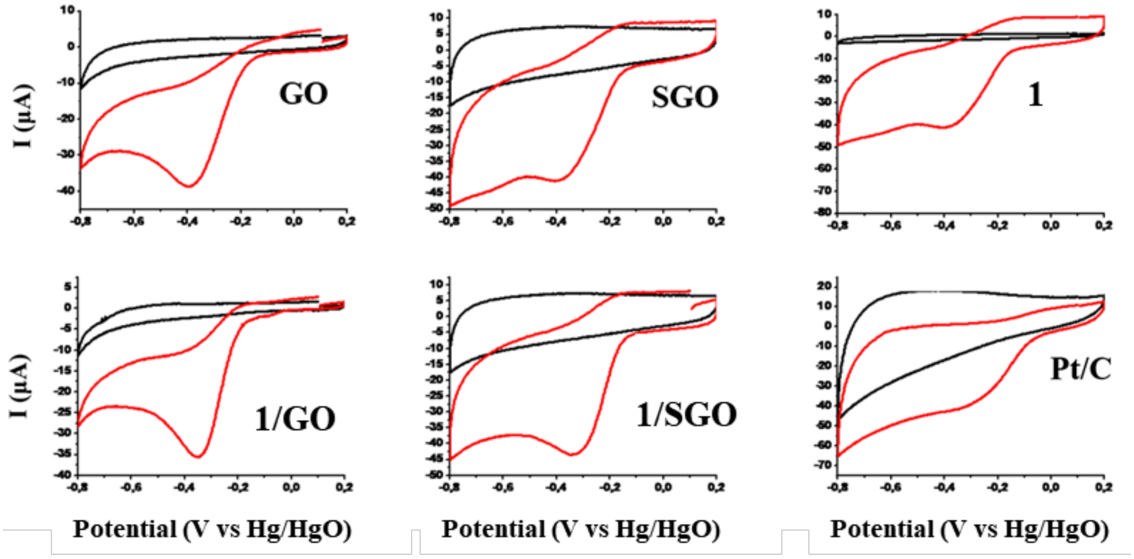

Figure S12. CV curves for **GO**, **SG**, **1**, **1/GO**, **1/SG** and commercial Pt/C in N_2 (black) and O_2 (red) saturated aqueous 0.1M KOH electrolyte.

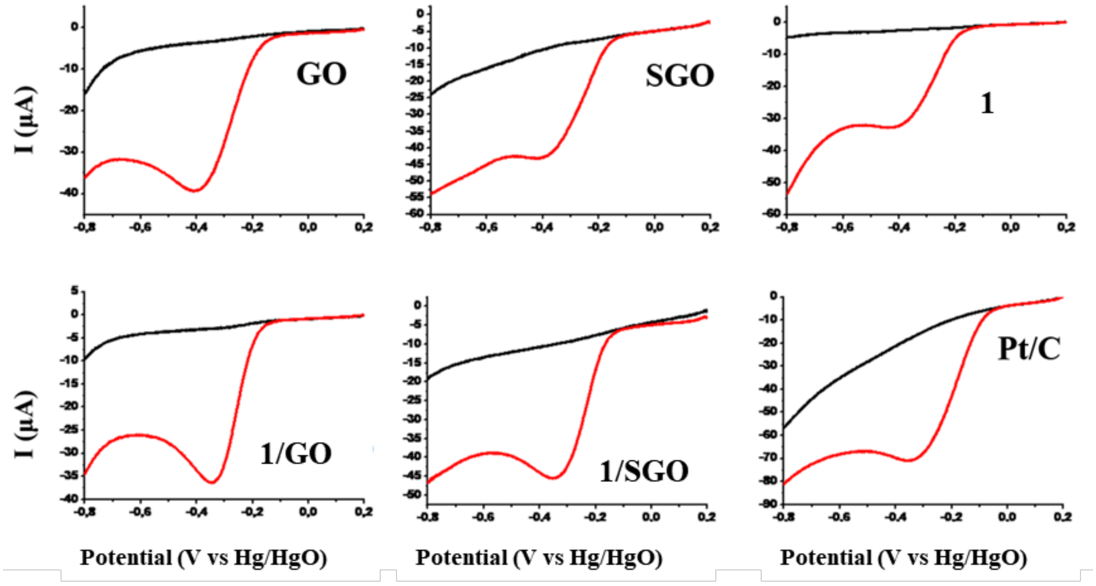

Figure S13. LSV curves for **GO**, **SG**, **1**, **1/GO**, **1/SG** and commercial Pt/C in N_2 (black) and O_2 (red) saturated aqueous 0.1M KOH electrolyte.

Table S1. Onset (E_{on}) and peak (E_p) reduction potentials of the electrocatalytic O_2 reduction derived from the CV and LSV curves recorded in O_2 saturated aqueous 0.1M KOH electrolyte and at a scan rate of 50 mV/s. All potentials are versus the Hg/HgO electrode, at 25^0C.

Material	**ORR E_{on} (CV)**	**ORR E_p (CV)**	**ORR E_{on} (LSV)**	**ORR E_p (LSV)**
1	-194mV	-391mV	-172mV	-386mV
GO	-181mV	-390mV	-172mV	-398mV
SG	-133mV	-377mV	-132mV	-383mV
1/GO	-179mV	-345mV	-184mV	-336mV
1/SG	-129mV	-320mV	-120mV	-327mV
Pt/C (5% Pt)	-76mV	-315mV	-78mV	-323mV

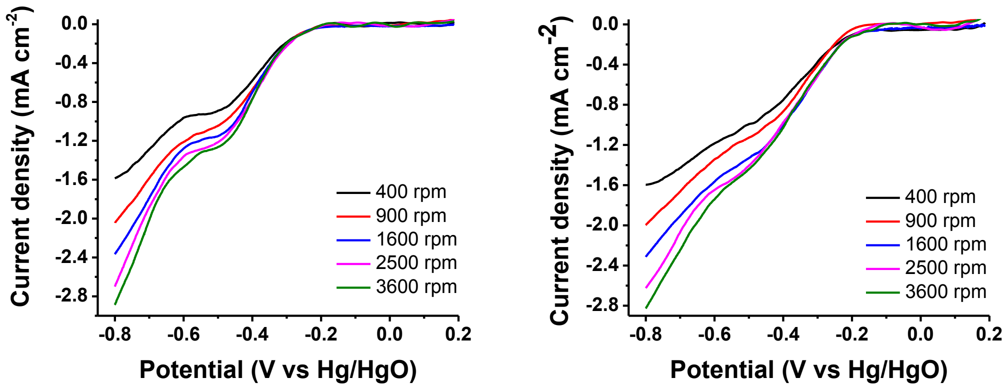

Figure S14.ORR polarization curves at 1600 rpm for **SG** (left panel) and **1/SG** (right panel) recorded in O_2 saturated aqueous 0.1M KOH electrolyte vs Hg/HgO.

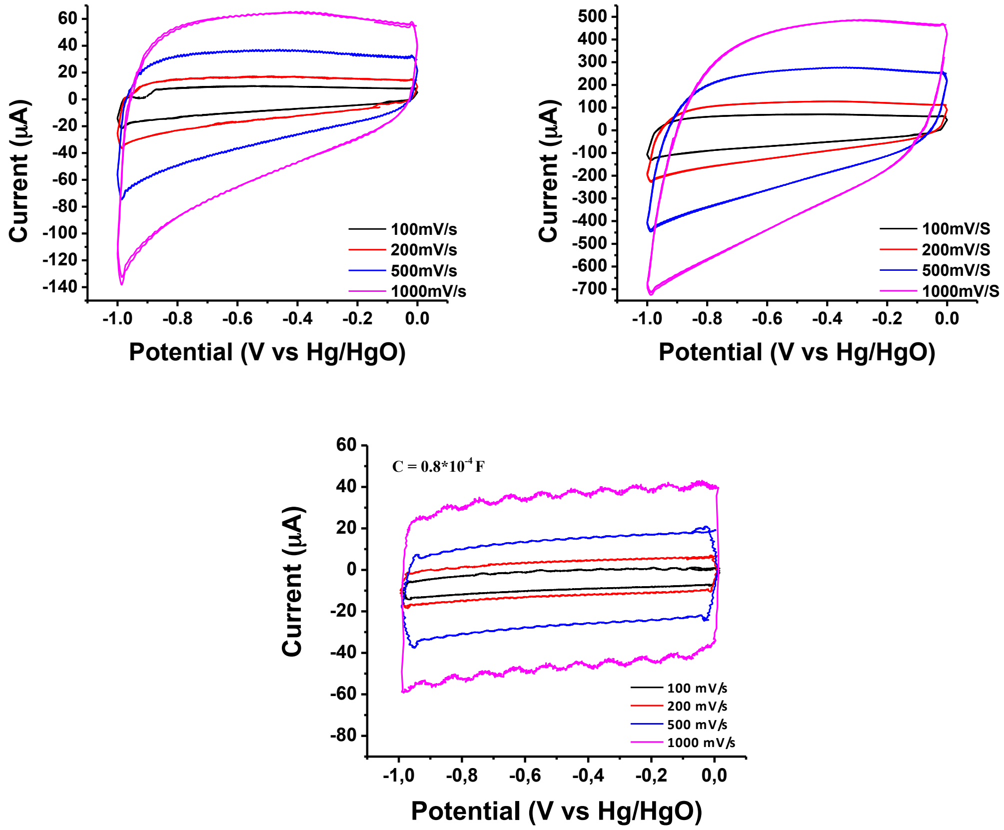

Figure S15. Capacitance curves for **SG** (up left panel), **1/SG** (up right panel) and **GO** (bottom panel) recorded in N_2 saturated aqueous 0.1M KOH electrolyte at different scan rates (0.1, 0.2, 0.5 and 1.0 V/s) vs Hg/HgO. The capacitance was calculated to be $0.8x10^{-4}$ for **GO**, $1.4x10^{-4}$ for **SG** and $9.5x10^{-4}$ F for **1/SG** ensembles, by integrating the average graph-area derived by the voltammographs in different scan rates.

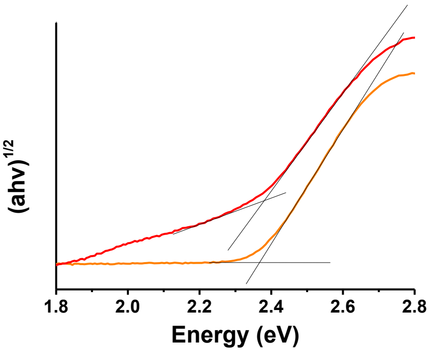

Figure S16. Tauc plots of **1/SG** (red) and **1** (orange) for calculating the band-gap.